Available online at www.sciencedirect.com
SCIENCE DIRECT®
Polymer 44 (2003) 6843–6850
polymer
www.elsevier.com/locate/polymer

Crystallization behavior of oxyethylene/oxybutylene diblock and triblock copolymers

Jun-Ting Xu[a,1], J. Patrick A. Fairclough[a], Shao-Min Mai[a], Chiraporn Chaibundit[b], M. Mingvanish[c], C. Booth[c], Anthony J. Ryan[a,*]

[a]*Department of Chemistry, The Polymer Centre, University of Sheffield, Sheffield S3 7HF, UK*
[b]*Polymer Science Program, Faculty of Science, Prince of Songkhla University, Songkhla 90112, Thailand*
[c]*Department of Chemistry, The University of Manchester, Manchester M13 9PL, UK*

Received 9 October 2002; received in revised form 26 May 2003; accepted 23 July 2003

Abstract

The crystallization behavior of poly(oxyethylene)-*b*-poly(oxybutylene) block copolymers with different compositions, morphologies and architectures (E_mB_n diblock copolymers and $E_mB_nE_m$, $B_nE_mB_n$ triblock copolymers) were investigated and the effect of volume fraction and architecture on the crystallization temperature (T_c) in non-isothermal crystallization was determined. It is found that the E_mB_n diblock copolymers having long E blocks exhibit similar crystallization temperatures, irrespective of volume fraction and morphology, but for the block copolymers with shorter E blocks the crystallization temperature increases with both the volume fraction, ϕ_E, and the length, m, of the E block. Some block copolymers with extremely low T_c, which fall into the temperature range normally associated with homogenous nucleation, were chosen for time-resolved small-angle X-ray scattering (SAXS) and isothermal crystallization kinetics experiments. The results show that breakout crystallization occurs in all these block copolymers. Therefore, unlike E_mB_n/B_h blends, there is no obvious relationship between T_c and crystallization behavior in neat block copolymers and homogeneous nucleation does not definitely lead to confined crystallization. The values of χ_c/χ_{ODT} for all the block copolymers with hex and bcc morphology were also calculated. It is found that all the block copolymers have $\chi_c/\chi_{ODT} < 3$, in agreement with the previously reported critical value and consistent with their breakout crystallization behavior.

Keywords: Block copolymer; Crystallization; Kinetics

1. Introduction

Recently confined crystallization of block copolymers has received much attention [1–9]. Confined crystallization (where crystallites are formed inside the original block copolymer morphology) is observed not only in crystalline/glassy block copolymers [1–3], but also in crystalline/rubbery block copolymers [4–9], whereas breakout crystallization (where the crystals erase the original block copolymer morphology) only occurs in ordered block copolymer melts. It has been found that confined and breakout crystallization show different nucleation mechanisms and crystallization temperatures. Confined crystallization usually leads to a homogeneous nucleation mechanism and a much lower crystallization temperature, as well as other characteristics, such as an Avrami exponent around 1, a smooth change of the *d*-spacing during non-isothermal crystallization and the preservation of morphology in the melt after crystallization [3–8]. However, the question whether homogeneous nucleation and confined crystallization are consequences of each other has not been unambiguously addressed. In a previous report [10] it was concluded that confined crystallization occurred based on only the low crystallization temperature from non-isothermal crystallization by DSC. In this paper, we present a wide range of data to show that a low crystallization temperature does not always lead to the conclusion that confined crystallization has occured.

It has been observed that both segregation strength and morphology affect crystallization in crystalline/rubbery block copolymers [6,8]. Loo et al. [5] attempted to classify

* Corresponding author.
[1] Permanent address: Department of Polymer Science and Engineering, Zhejiang University, Hangzhou 310027, China.

0032-3861/$ - see front matter © 2003 Elsevier Ltd. All rights reserved.
doi:10.1016/S0032-3861(03)00690-6

crystallization behavior of this type block copolymer based on the map of relative segregation strength, given by $(\chi N_t)_c/(\chi N_t)_{ODT}$ (where χ is the Flory Huggins interaction parameter; N_t, the volume averaged degree of polymerization; the subscripts c and ODT refer to the crystallization and order–disorder temperature, respectively) versus volume fraction. In polyethylene-*b*-poly(styrene-*r*-ethylene-*r*-butene) (E/SEB) and polyethylene-*b*-poly(3-methyl-1-butylene) (E/MB) block copolymers, they found that confined crystallization occurs at $(\chi N_t)_c/(\chi N_t)_{ODT} > 3$ and below $(\chi N_t)_c/(\chi N_t)_{ODT} = 3$ crystallization breaks out. We applied a similar index χ_c/χ_{ODT} for the poly(oxyethylene)-*b*-poly(oxybutylene)/poly(oxybutylene) (E_mB_n/B_h) blends, assuming that the changes of N_t with temperature are the same for E and B segments, and found that confined and breakout crystallization can also be separated by the line of $\chi_c/\chi_{ODT} = 3$ [7]. Therefore, it appears that this classification could be generalized to different block copolymer systems. We have synthesized a series of oxyethylene/oxybutylene block copolymers with different compositions, morphologies and architectures including E_mB_n diblock copolymers, $E_mB_nE_m$ and $B_nE_mB_n$ triblock copolymers and the solid and melt structures have been intensively investigated [11–16]. In this paper, we study crystallization behavior (breakout or confined crystallization) and the crystallization temperatures of a range of oxyethylene/oxybutylene block copolymers. The classification of crystallization behavior using relative segregation strength is also tested in neat oxyethylene/oxybutylene block copolymers with different architectures.

2. Experimental

2.1. Materials

The E_mB_n diblock and $E_mB_nE_m$, $B_nE_mB_n$ triblock copolymers (where the subscripts m and n refer to the average polymerization degree of oxyethylene and oxybutylene, respectively) were synthesized using sequential anionic polymerization and have been described elsewhere [12–14]. All the block copolymers have narrow molecular weight distributions ($M_w/M_n < 1.05$) measured by GPC. The composition of the block copolymers was determined by solution-state ^{13}C NMR employing chloroform as solvent.

2.2. DSC experiments

The DSC experiments were carried out using a Perkin–Elmer Pyris-1 calorimeter. In non-isothermal crystallization processes, the block copolymers were first heated to 80 °C and held for 5 min then cooled from the melt to −50 °C at a rate of 10 °C/min. The peak temperature was taken as crystallization temperature (T_c). In isothermal crystallization, the block copolymers were held in the molten state for 5 min, and then cooled down at a rate of 100 °C/min to the crystallization temperatures and held until crystallization was completed. The change of heat flow with time was recorded upon crystallization. The isothermal crystallization kinetics of polymer can be analyzed using the Avrami equation [17]

$$1 - X(t) = \frac{\Delta H^c_{t=\infty} - \Delta H^c_t}{\Delta H^c_{t=\infty} - \Delta H^c_{t=0}} = \exp(-kt^n) \quad (1)$$

where $X(t)$ is the relative crystallinity at time t, $\Delta H^c_{t=\infty}$ and ΔH^c_t are the crystallization enthalpies on complete crystallization and after time t. Therefore, we have:

$$\log[-\ln(1 - X(t))] = \log k + n \log t \quad (2)$$

The crystallization rate constant k and Avrami exponent n can be determined from the intercept and slope in the plot of $\log[-\ln(1 - X(t))]$ versus $\log(t)$.

2.3. Time-resolved small angle X-ray scattering

The simultaneous time-resolved SAXS/DSC experiments were carried out on beamline 8.2 of the SRS at the Daresbury, Warrington, UK. The selected samples were first heated to erase the crystalline structure, a temperature above the melting point of the E block but below the ODT (depending on the polymer to a maximum of 80 °C), then cooled at a rate of 10 °C/min to complete crystallization. The samples were then subsequently heated at rate of 10 °C/min until the order–disorder transition was observed. The data were collected in 10 s frames separated by a waiting-time of 10 μs. Details of the instrument and data processing are described elsewhere [12,13].

2.4. Optical microscopy

Optical microscopy experiments were conducted on an Olympus BX50 microscope connected to a Panasonic NV-HD660 video recorder with a Linkam optical DSC equipped with a liquid N_2 cooling system. Samples with ~1 μm thickness were kept in the molten state for 5 min, subsequently the samples were cooled down to the crystallization temperature at a rate of 100 °C/min and held until crystallization was completed. The texture of the block copolymers during crystallization was recorded.

3. Results

3.1. Crystallization temperature (T_c) in non-isothermal crystallization

The crystallization temperatures (T_c) in non-isothermal crystallization for E_mB_n diblock copolymers, $E_mB_nE_m$ and $B_nE_mB_n$ triblock copolymers are summarized in Table 1.

Table 1
Characteristics and properties of block copolymers

Copolymer	ϕ_E	Structure in melt	T_c^a (°C)	χ_c	T_{ODT} (°C)	χ_{ODT}	χ_c/χ_{ODT}
$E_{40}B_{70}$	0.210	bcc	−19.3	0.219	60	0.140	1.56
$E_{47}B_{62}$	0.286	hex	14.9	0.180	93	0.118	1.53
$E_{50}B_{70}$	0.270	hex	15.3	0.179	112	0.106	1.69
$E_{64}B_{60}$	0.361	hex	23.0	0.172	126	0.099	1.74
$E_{68}B_{65}$	0.356	hex	23.9	0.171	140	0.092	1.86
$E_{75}B_{54}$	0.424	gyr	22.3/28.3(m)[b]	0.167	126	0.099	1.69
$E_{85}B_{45}$	0.497	lam	32.3	0.163	140	0.092	1.77
$E_{100}B_{51}$	0.509	lam	21.9/33.6(m)[b]	0.162	165	0.080	2.02
$E_{110}B_{30}$	0.660	lam	36.6	0.160	85	0.123	1.30
$E_{114}B_{56}$	0.519	lam	37.3	0.159	210	0.062	2.56
$E_{115}B_{103}$	0.371	hex	38.3	0.158	225	0.057	2.77
$E_{131}B_{35}$	0.664	lam	39.6	0.157	133	0.095	1.65
$E_{150}B_{256}$	0.235	n.c.[c]	38.3	0.158	109	0.108	1.46
$E_{155}B_{76}$	0.519	lam	40.2	0.156	270	0.043	3.63
$E_{56}B_{27}$	0.523	lam	28.3/30.9(m)[b]	0.165	53[d]	0.146	1.13
$E_{35}B_{12}$	0.607	dis	20.7		–	–	–
$E_{35}B_{114}E_{35}$	0.245	hex	−28.2	0.231	125	0.099	2.33
$E_{34}B_{75}E_{83}$	0.324	hex	9.3(m)/24.9[b]	0.186	113	0.106	1.75
$E_{31}B_{54}E_{31}$	0.378	lam	11.0(m)/23.9[b]	0.184	74	0.130	1.41
$E_{43}B_{100}E_{43}$	0.313	hex	−23.7/11.9(m)[b]	0.183	148	0.088	2.08
$E_{53}B_{86}E_{53}$	0.395	hex	16.3(m)/22.6[b]	0.179	141	0.091	1.97
$E_{48}B_{100}E_{48}$	0.337	hex	17.8	0.177	153	0.085	2.08
$E_{38}B_{38}E_{38}$	0.514	lam	18.3	0.176	46[d]	0.151	1.17
$E_{71}B_{79}E_{71}$	0.487	gyr	26.9	0.168	153	0.085	1.98
$E_{65}B_{59}E_{65}$	0.538	lam	28.9	0.166	124	0.100	1.66
$E_{72}B_{68}E_{72}$	0.528	lam	29.3	0.166	140	0.092	1.80
$E_{103}B_{86}E_{103}$	0.559	lam	24.6/32.6(m)[b]	0.163	219	0.059	2.76
$E_{89}B_{103}E_{89}$	0.478	lam	34.9	0.161	207	0.063	2.56
$E_{91}B_{56}E_{91}$	0.632	lam	36.6	0.159	139	0.092	1.73
$B_{65}E_{75}B_{64}$	0.235	bcc	−21.0	0.222	86	0.122	1.82
$B_{49}E_{63}B_{49}$	0.254	bcc	−18.8	0.219	55	0.134	1.63
$B_{37}E_{77}B_{37}$	0.355	hex	12.9	0.182	72	0.122	1.49
$B_{19}E_{58}B_{19}$	0.447	dis	16.6	–	–	–	–
$B_{34}E_{93}B_{34}$	0.42	gyr	20.7	0.174	72	0.132	1.32
$B_{46}E_{99}B_{46}$	0.363	hex	21.3	0.173	120	0.102	1.70
$B_{24}E_{79}B_{24}$	0.465	dis	22.6	–	–	–	–
$B_{14}E_{56}B_{14}$	0.514	dis	23.0	–	–	–	–
$B_{44}E_{127}B_{44}$	0.433	hex	24.6	0.170	129	0.097	1.75
$B_{29}E_{111}B_{29}$	0.503	lam	27.9	0.167	90	0.120	1.39
$B_{36}E_{137}B_{36}$	0.502	lam	28.6	0.167	134	0.095	1.76
$B_{37}E_{150}B_{37}$	0.517	lam	23.3/30.9(m)[b]	0.165	143	0.090	1.83
$B_{25}E_{143}B_{25}$	0.602	lam	23.3/33.3(m)[b]	0.162	88	0.121	1.34
$B_{28}E_{182}B_{28}$	0.632	lam	35.9	0.160	83	0.124	1.29

[a] The crystallization temperatures reported are the result of programmed cooling of the sample at 10 °C/min.
[b] Double crystallization peaks are observed and m denotes the major peak.
[c] Not clear because of multiple first-order peaks.
[d] Disorder–order transition temperature.

We choose this programmed cooling method of screening the onset of crystallization to try to differentiate between the different modes of crystallization. Fig. 1 shows the plot of T_c of E_mB_n diblock copolymers versus volume fraction of the E block. It is observed that six diblock copolymers ($E_{110}B_{30}$, $E_{114}B_{56}$, $E_{115}B_{103}$, $E_{131}B_{35}$, $E_{150}B_{256}$, $E_{155}B_{75}$) have similar crystallization temperatures (guided by the horizontal line in Fig. 1), though ϕ_E ranges from 0.235 to 0.664 and the morphologies of all these six diblock copolymers are different. This shows that the T_c of the diblock copolymers is independent of the volume fraction and morphology as long as the E block is long enough (probably $m^* \geq 110$) to form crystals at high temperatures with a small number of folds (~3). Such thick crystals can more readily span domains, allowing secondary nucleation of crystallization to proceed from domain to domain, following an initial heterogeneous nucleation event. This behavior is in contrast to the behavior of polyolefin block copolymers [5] where the crystal thickness is dominated by the microstructure of the crystallizable block and there are no appreciable effects of the block length on the crystallization temperature for a given segregation strength. In these E_mB_n block copolymers

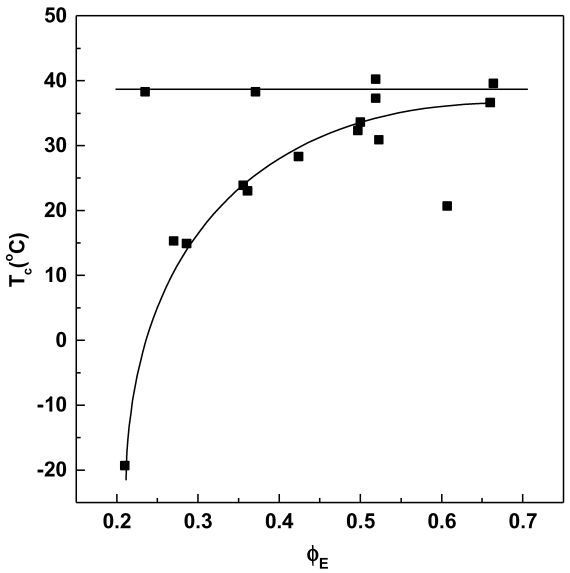

Fig. 1. T_c in non-isothermal crystallization (programmed cooling at 10 °C/min) versus volume fraction of the E block for E_mB_n diblock copolymers. The solid lines guide the eye to two types of change of T_c with ϕ_E.

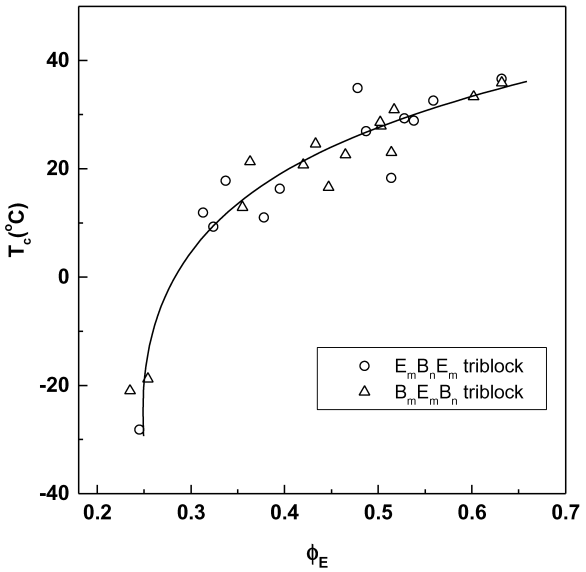

Fig. 2. T_c in non-isothermal crystallization (programmed cooling at 10 °C/min) versus volume fraction of the E block for $E_mB_nE_m$ and $B_nE_mB_n$ triblock copolymers. The solid line is a guide to the eye.

the crystal thickness makes them more susceptible to heterogeneous nucleation at higher block lengths and at high E length the melting point is similarly insensitive to the volume fraction. For the diblock copolymers with shorter E blocks, the T_c increases with volume fraction of E block (guided by the curve in Fig. 1). Especially at low E volume fraction, the T_c is strongly depressed. For example, the diblock copolymer $E_{40}B_{79}$ with $\phi_E = 0.21$ and a bcc morphology has a very low T_c of -19.3 °C. We also notice that, if the E block is very short, such as $E_{35}B_{12}$, the diblock copolymer may have a still lower T_c, even though the volume fraction of E is high.

The variations of T_c with volume fraction of E for $E_mB_nE_m$ and $B_nE_mB_n$ triblock copolymers are shown in Fig. 2. Since m^* ($m^* = m$ for $E_mB_nE_m$ and $m^* = m/2$ for $B_nE_mB_n$ [18]) is less than 110 in all triblock copolymers, the crystallization temperatures are all dependent on volume fraction. It is found that the T_c of triblock copolymers increases with volume fraction of E.

The plot of T_c versus m^* is shown in Fig. 3. We can see that the crystallization temperatures of all these three block copolymer architectures change with m^* in a similar way. The crystallization temperature basically increases with the length of E block when the E block is below the critical length, but such dependence is weaker for block copolymers with longer E block. It is also observed that the some block copolymers with short E block shows large differences in T_c, indicating a strong dependence of T_c on volume fraction, as shown in Fig. 2.

The results reveal that both volume fraction and the length of the E block have an influence on the T_c of oxyethylene/oxybutylene block copolymers. Therefore, we try to find a general relationship between T_c, volume fraction and m^*. It is observed that the data fall into a universal curve when $\ln(T_c)$ is plotted with $\ln[(\phi_E - \phi_E^{crit})^2(m^* - m^*_{crit})]$ (Fig. 4), where the critical values of ϕ_E and m^* are estimated to be $\phi_E^{crit} = 0.20$ and $m^*_{crit} = 26$ from fitting the data for the variation of T_c with ϕ_E and m^*. The four block copolymers with extremely low T_c, however, still deviate from this universal scaling line.

3.2. SAXS

The data in Table 1 show that most of the block copolymers have higher T_c when compared with the E_mB_n/

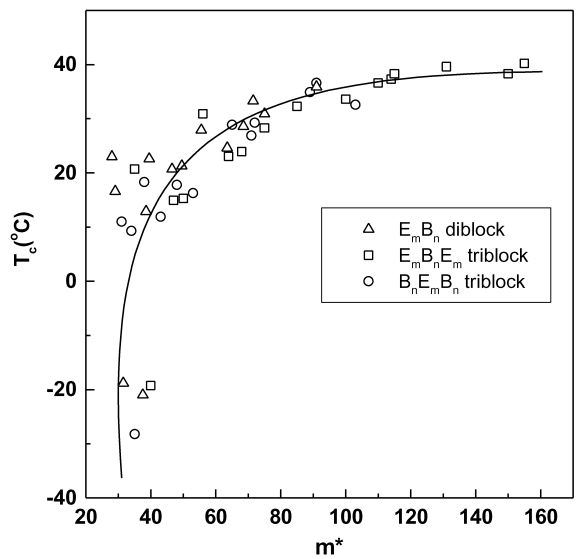

Fig. 3. T_c in non-isothermal crystallization (programmed cooling at 10 °C/min) versus m^* for E_mB_n diblock copolymers and $E_mB_nE_m$, $B_nE_mB_n$ triblock copolymers. ($m^* = m$ for E_mB_n and $E_mB_nE_m$, and $m^* = m/2$ for $B_nE_mB_n$.)

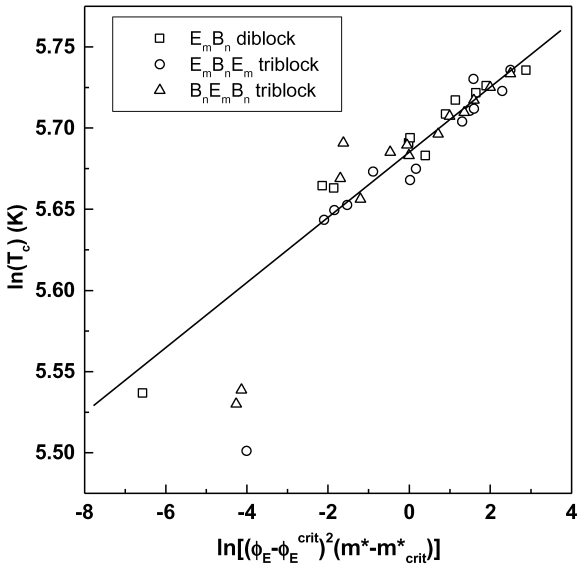

Fig. 4. Relationship between T_c, m^* and volume fraction. ($m^* = m$ for E_mB_n and $E_mB_nE_m$, and $m^* = m/2$ for $B_nE_mB_n$.)

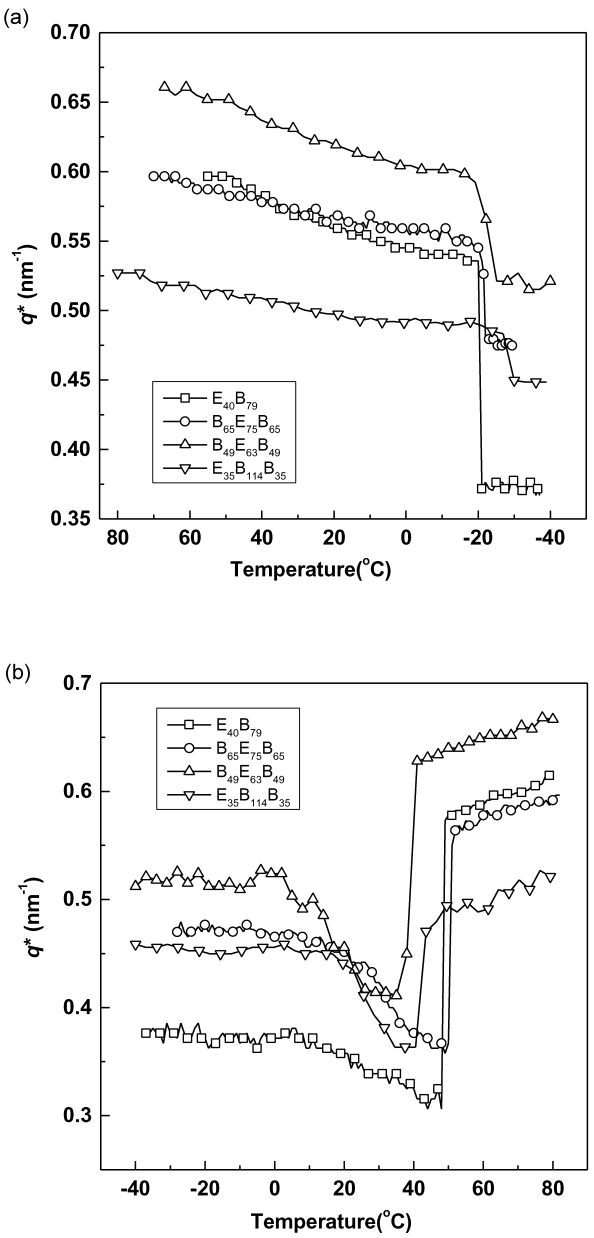

Fig. 5. Change of q^* during non-isothermal crystallization (a) and melting (b). The cooling and heating rates are 10 °C/min.

B_h blends with confined crystallization [6], indicating breakout crystallization of these block copolymers. However, we also notice that the crystallization temperature of some block copolymers, such as $E_{40}B_{79}$ (−19.3 °C), $E_{35}B_{114}E_{35}$ (−28.2 °C), $B_{65}E_{75}B_{65}$ (−21 °C) and $B_{49}E_{63}B_{49}$ (−18.8 °C), are very low crystallization temperatures in non-isothermal crystallization, which have fallen into the temperature range where homogeneous nucleation is normally observed. Our previous studies on E_mB_n/B_h blends [6] revealed that homogeneous nucleation is usually related to confined crystallization. As a result, these four block copolymers were selected for time-resolved SAXS characterization to study their non-isothermal crystallization and melting behavior. As previously reported [6], confined or breakout crystallization can be inferred from the change of q^* with temperature during crystallization. If q^* varies smoothly with temperature, crystallization is confined within the original block copolymer morphology. Otherwise, crystallization breaks out of the original block copolymer morphology to form lamellae and q^* shows a stepwise change. The changes of q^* during non-isothermal crystallization and melting for these four block copolymers are depicted in Fig. 5. Surprisingly, a stepwise change of q^* after crystallization is observed in all these four samples (Fig. 5a), indicating breakout crystallization. The melting behavior leads to the same conclusion. A common feature in the melting behavior is observed for these four block copolymers: q^* decreases gradually before complete melting followed by a stepwise increase after melting (Fig. 5b), these are the melting characteristic of lamellar crystals and indicates a lamellar structure in the solid [19]. Fig. 6 is an example of three-dimensional SAXS profiles for $E_{40}B_{79}$ during non-isothermal crystallization. As we can see, the first peak is displaced after crystallization and the morphology is transformed from a spherical morphology in the melt into lamellar structure in the solid.

3.3. Isothermal crystallization kinetics

Isothermal crystallization kinetics have also been used to distinguish confined crystallization from breakout crystallization. Confined crystallization is initiated by homogeneous nucleation and the crystallization rate is controlled by nucleation rate, leading to an Avrami exponent around 1 [1,3,7]. In contrast, breakout crystallization involves secondary nucleation spanning different domains, and generally has an Avrami exponent from 2 to 4. The isothermal crystallization parameters obtained for $E_{40}B_{79}$,

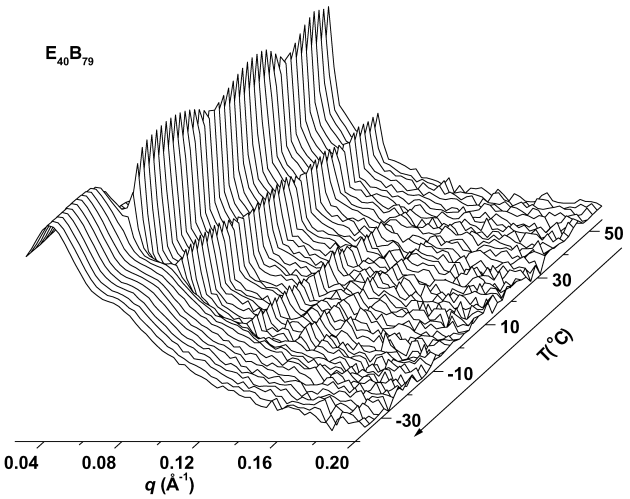

Fig. 6. Three-dimensional SAXS profiles of log $I(q,t)$ versus q versus t for $E_{40}B_{79}$ on cooling from the melt at a rate of 10 °C/min.

$E_{35}B_{114}E_{35}$ and $B_{49}E_{63}B_{49}$ are given in Table 2. It is found that all block copolymers have Avrami exponents considerably larger than 1, indicating breakout crystallization. As a result, the isothermal crystallization kinetics leads to the same conclusion as SAXS. The micrographs in Fig. 7 show the change of morphology with crystallization time for $B_{49}E_{63}B_{49}$ crystallized at −4 °C. Spherulites with a Maltese cross are observed. The movement of the crystallization front and the impingement of spherulites at late crystallization stage can also be readily monitored by optical microscopy. This clearly reveals breakout crystallization in this block copolymer, since in confined crystallization the domains are nano-scale and smaller than wavelength of light, and the block copolymers are transparent after crystallization.

Table 2
Isothermal crystallization parameters for selected block copolymers

Copolymer	T_c (°C)	log k	Avrami exponent (n)
$E_{40}B_{79}$ ($\phi_E = 0.210$)	−10	−3.4	1.9
	−8	−3.5	2.0
	−6	−3.9	2.2
	−4	−4.6	2.8
$E_{35}B_{114}E_{35}$ ($\phi_E = 0.245$)	−20	−7.3	3.4
	−18	−8.1	3.7
	−16	−8.5	3.8
	−14	−8.8	3.7
$B_{49}E_{63}B_{49}$ ($\phi_E = 0.254$)	−10	−4.6	2.6
	−8	−5.7	2.9
	−6	−6.9	2.7
	−4	−7.1	3.1
$B_{65}E_{75}B_{65}$ ($\phi_E = 0.235$)	−10	−5.3	3.1
	−8	−7.2	3.7
	−6	−7.8	3.5
	−4	−8.8	3.5

4. Discussion

The results above show that in neat oxyethylene/oxybutylene block copolymers the programmed cooling crystallization temperature cannot be used to judge whether crystallization has been confined by or has broken out of the melt morphology. However, for the E_mB_n/B_h blends we have found that the crystallization temperature is a good indicator of the crystallization behavior, that is confinement or breakout. We speculate that this difference results from the significant influence of composition and structure on the T_c in neat block copolymers since all the B segments are connected to an E block, the mobility of the E block is remarkably reduced, especially at low ϕ_E. As a result, crystallization initiated by heterogeneous nucleation proceeds very slowly and the crystals formed by heterogeneous nucleation only accounts for a small fraction of domains, during programmed cooling, before the temperature falls into the homogeneous nucleation region. However, cooperative crystallization of different E domains initiated by homogeneous nucleation can also lead to breakout of the morphology. The block copolymers used in E_mB_n/B_h blends, thus far, all have $\phi_E \sim 0.5$. As can be seen from Fig. 1, at such a ϕ_E the B block has little influence on T_c, provided the E block is sufficiently long to form thick crystals at high temperatures with a small number of folds. Such thick crystals can more readily span domains allowing secondary nucleation of crystallization to proceed from domain to domain following an initial heterogeneous nucleation event. On the other hand, in the blends all the crystallizable E blocks are in block copolymers and the mobility of the E block is increased because the amorphous B homopolymer is not connected with the E blocks. In order to further examine the effect of the B block on T_c, we use two E_mB_n diblock copolymers $E_{114}B_{56}$ and $E_{115}B_{103}$, which have similar E length but different B length, to make a series of blends with the same ϕ_E. The changes of T_c with ϕ_E are shown in Fig. 8. The blends with a longer B-block ($E_{115}B_{103}/B_{28}$) exhibit a lower T_c than the blends with a shorter B-block ($E_{114}B_{56}/B_{28}$) at the same ϕ_E. A corollary of this is that a block copolymer E_mB_n would have a lower T_c than any blend at the same the same E length and ϕ_E and is entirely consistent with the stronger segregation (i.e. higher T_{ODT}) of the neat copolymers versus the blends.

We have also blended block copolymers of different architectures with amorphous homopolymer and compare the T_c of the blends with those of the neat block copolymers having similar E length and ϕ_E. The results are listed in Table 3. It is found that the crystallization temperatures of the neat block copolymers, which have the longer B block connected to the E block, are generally lower than those of corresponding blends with a shorter connected B block, though, surprisingly the melting temperatures and d-spacing of the neat block copolymers are higher. The T_m data implies that the E-crystals in the block copolymers are thicker than those in the blend, this is confirmed by the d-

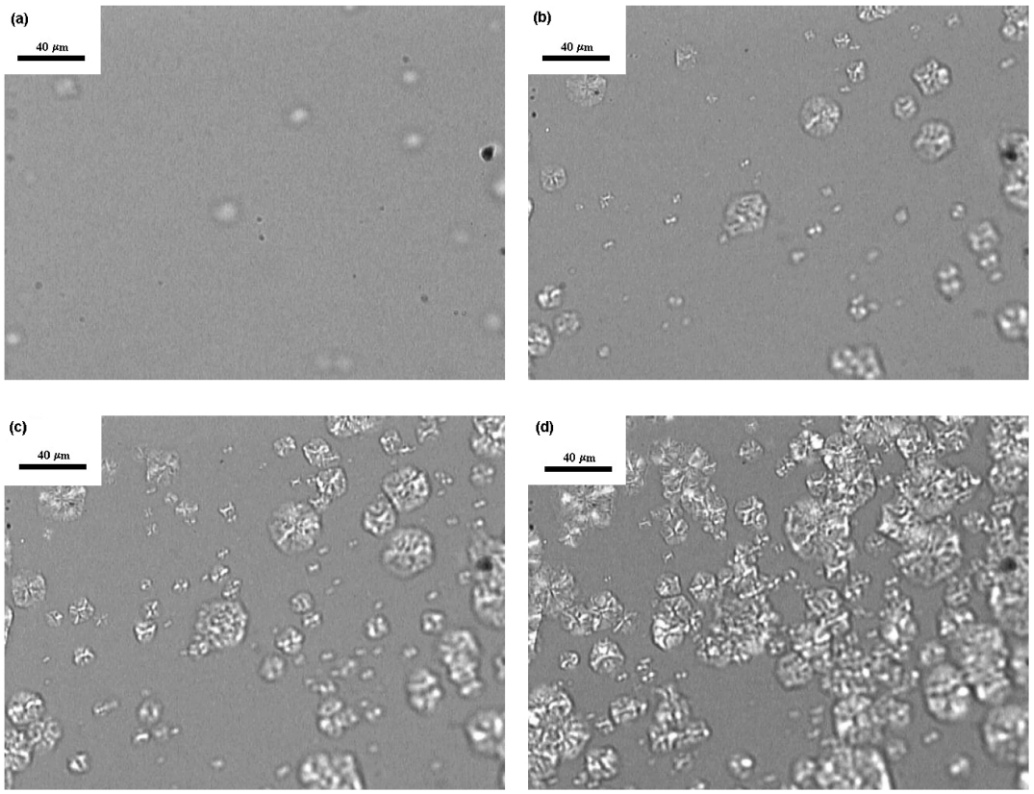

Fig. 7. Optical micrographs of $B_{49}E_{63}B_{49}$ crystallized at −4 °C. for (a) 0.5 min; (b) 1.5 min; (c) 4.0 min and (d) 7.0 min.

spacings, and is not what might be intuitively expected from the lower T_c. The neat diblocks are more highly confined (further from the ODT) than the blends and less mobile, the connected amorphous block reduces the overall mobility of the block copolymer. Moreover, the entropy change on crystallization of the blend and its corresponding block copolymer are obviously rather different, given that at equilibrium $\Delta H/T_c = \Delta S$ and the enthalpy of crystallization is effectively constant. On crystallization, the B block in the neat block copolymer is significantly stretched, a larger ΔS, whereas the attached B-block in the blend need not perturb its configuration particularly given the prescence of the homopolymer B, it is the entropic piston of the attached B block that drives down T_c.

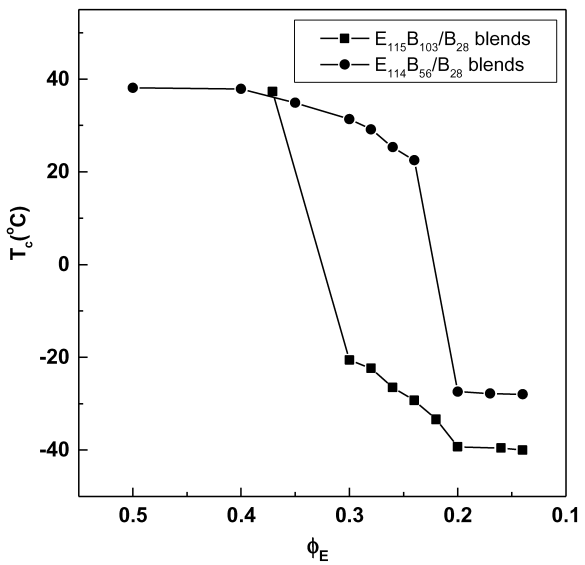

Fig. 8. Comparison of crystallization temperatures (T_c) for $E_{114}B_{56}/B_{28}$ and $E_{115}B_{103}/B_{28}$ blends as a function of the volume fraction of the crystallizable block.

The study of the crystallization temperatures of the neat oxyethylene/oxybutylene block copolymers reveals, therefore, that homogeneous nucleation does not necessarily give rise to confined crystallization. Confined crystallization is definitely initiated by homogeneous nucleation, but homogeneous nucleation does not always lead to confined crystallization. Confined or breakout crystallization can

Table 3
Comparison of the T_c and T_m of some neat block copolymers and blends

Samples	ϕ_E	T_c (°C)	T_m (°C)	d (Å)[a]
$E_{50}B_{70}$	0.270	15.3	44.0	214
$E_{56}B_{27}/B_{14}$	0.270	16.2	40.0	206
$E_{35}B_{114}E_{35}$	0.245	−28.2	46.2	140
$E_{38}B_{38}E_{38}/B_{14}$	0.245	6.6	35.5	132
$E_{43}B_{100}E_{43}$	0.313	−23.7/11.9(m)	48.4	–
$E_{51}B_{50}E_{51}/B_{14}$	0.313	22.8	45.5	–
$B_{65}E_{76}B_{65}$	0.237	−21.0	42.0	136
$B_{37}E_{77}B_{37}/B_{14}$	0.237	−16.8	35.5	130
$B_{46}E_{99}B_{46}$	0.363	21.3	48.3	–
$B_{26}E_{96}B_{26}/B_{14}$	0.363	21.7	41.8	–

[a] After crystallization.

only be assessed by SAXS or isothermal crystallization kinetics, but not solely by the programmed cooling crystallization temperature or nucleation mechanism alone.

Our previous work shows that the crystallization behavior of E_mB_n/B_h blends with bcc and hex morphologies can be classified using relative segregation strength χ_c/χ_{ODT} [7]. When χ_c/χ_{ODT} is larger than 3, crystallization is confined, whereas breakout crystallization takes place in the blends with $\chi_c/\chi_{ODT} < 3$. In order to test whether this hypothesis is applicable to neat oxyethylene/oxybutylene block copolymers of different architectures, the values of χ_c/χ_{ODT} for block copolymers are also calculated and are listed in Table 1. The parameter χ at the order–disorder transition temperature (T_{ODT}) and crystallization temperature (T_c) was estimated by [18]:

$$\chi = 84.1/T - 0.112 \quad (3)$$

It is found that $\chi_c/\chi_{ODT} < 3$ for all the block copolymers with bcc and hex morphologies, which is in accordance with our observation of breakout crystallization. As a result, the classification of confined and breakout crystallization using relative segregation strength χ_c/χ_{ODT} still holds for simple oxyethylene/oxybutylene diblock and triblock copolymers at present. Nevertheless, we have not yet managed to synthesize an oxyethylene/oxybutylene block copolymers having hex or bcc morphology with $\chi_c/\chi_{ODT} > 3$ and we cannot test such a classification on oxyethylene/oxybutylene block copolymers showing confined crystallization behavior.

5. Conclusions

We have revealed that both composition and architecture affect the crystallization temperature of oxyethylene/oxybutylene block copolymers in programmed cooling, non-isothermal crystallization. When the E block is short and the volume fraction ϕ_E is small, the block copolymers may exhibit extremely low crystallization temperatures, which fall into the temperature range normally associated with homogeneous nucleation. However, the time-resolved SAXS, isothermal crystallization kinetics and optical microscopy experiments show that breakout crystallization still occurs in such block copolymers with low crystallization temperatures. This means that homogeneous nucleation does not definitely lead to confined crystallization, though confined crystallization is normally a result of homogeneous nucleation. All the block copolymers with hex and bcc morphology in the present work have values of $\chi_c/\chi_{ODT} < 3$, in accordance with their breakout crystallization behavior. Thus the classification of confined and breakout crystallization with relative segregation strength still holds true in oxyethylene/oxybutylene block copolymers with different architectures.

Acknowledgements

JX was supported by The Board of Pao Yu-kong and Pao Zhao-long Scholarship and Dow Chemicals during his stay at the University of Sheffield, SMM was supported by EPSRC Grant GR/L22621. Beamtime at Daresbury was provided under EPSRC Grant GR/M22116.

References

[1] Zhu L, Mimnaugh BR, Ge Q, Quirk RP, Cheng SZD, Thomas EL, Lotz B, Hsiao BS, Yeh F, Liu LZ. Polymer 2001;42:9121.
[2] Zhu L, Chen Y, Zhang AQ, Calhoun BH, Chun MS, Quirk RP, Cheng SZD, Hsiao BS, Yeh FJ, Hashimoto T. Phys Rev B: Condens Matter 1999;60:10022.
[3] Loo YL, Register RA, Ryan AJ, Dee GT. Macromolecules 2001;34:8968.
[4] Loo YL, Register RA, Ryan AJ. Phys Rev Lett 2000;84:4120.
[5] Loo YL, Register RA, Ryan AJ. Macromolecules 2002;35:2365.
[6] Xu JT, Turner SC, Fairclough JPA, Mai SM, Ryan AJ, Chaibundit C, Booth C. Macromolecules 2002;35:3614.
[7] Xu JT, Fairclough JPA, Mai SM, Ryan AJ, Chaibundit C. Macromolecules 2002;35:6937.
[8] Chen HL, Hsiao SC, Lin TL, Yamauchi K, Hasegawa H, Hashimoto T. Macromolecules 2001;34:671.
[9] Chen HL, Wu JC, Lin TL, Lin JS. Macromolecules 2001;34:6936.
[10] Muller AJ, Balsamo V, Arnal ML, Jakob T, Schmalz H, Abetz V. Macromolecules 2002;35:3048.
[11] Ryan AJ, Fairclough JPA, Hamley IW, Mai SM, Booth C. Macromolecules 1997;30:1723.
[12] Mai SM, Fairclough JPA, Viras K, Gorry PA, Hamley IW, Ryan AJ, Booth C. Macromolecules 1997;30:8392.
[13] Mai SM, Fairclough JPA, Terrill NJ, Turner SC, Hamley IW, Matsen MW, Ryan AJ, Booth C. Macromolecules 1998;31:8110.
[14] Mai SM, Mingvanish W, Turner SC, Chaibundit C, Fairclough JPA, Heatley F, Matsen MW, Ryan AJ, Booth C. Macromolecules 2000;33:5124.
[15] Chaibundit C, Mingvanish W, Turner SC, Mai SM, Fairclough JPA, Ryan AJ, Matsen MW, Booth C. Macromol Rapid Commun 2000;21:964.
[16] Chaibundit C, Mingvanish W, Booth C, Mai SM, Turner SC, Fairclough JPA, Ryan AJ, Pissis P. Macromolecules 2002;35:4838.
[17] Avrami M. J Chem Phys 1939;7:1103.
[18] Ryan AJ, Mai SM, Fairclough JPA, Hamley IW, Booth C. Phys Chem Chem Phys 2001;3:2961.
[19] Ryan AJ, Stanford JL, Bras W, Nye TMW. Polymer 1997;38:759.